

See discussions, stats, and author profiles for this publication at: <https://www.researchgate.net/publication/271773681>

Extracellular synthesis of gold bionanoparticles by *Nocardioopsis* sp. and evaluation of its antimicrobial, antioxidant and cytotoxic activities

ARTICLE in BIOPROCESS AND BIOSYSTEMS ENGINEERING · FEBRUARY 2015

Impact Factor: 2 · DOI: 10.1007/s00449-015-1358-y

CITATIONS

3

READS

171

5 AUTHORS, INCLUDING:



Panchanathan Manivasagan

Pukyong National University

42 PUBLICATIONS 245 CITATIONS

SEE PROFILE



Moch Syaiful Alam

Pukyong National University

1 PUBLICATION 3 CITATIONS

SEE PROFILE



Kyong-Hwa Kang

Pukyong National University

30 PUBLICATIONS 160 CITATIONS

SEE PROFILE

Extracellular synthesis of gold bionanoparticles by *Nocardiopsis* sp. and evaluation of its antimicrobial, antioxidant and cytotoxic activities

Panchanathan Manivasagan · Moch Syaiful Alam ·
Kyong-Hwa Kang · Minseok Kwak ·
Se-Kwon Kim

Received: 12 November 2014 / Accepted: 9 January 2015
© Springer-Verlag Berlin Heidelberg 2015

Abstract Advancement of biological process for the synthesis of bionanoparticles is evolving into a key area of research in nanotechnology. The present study deals with the biosynthesis, characterization of gold bionanoparticles by *Nocardiopsis* sp. MBRC-48 and evaluation of their antimicrobial, antioxidant and cytotoxic activities. The gold bionanoparticles obtained were characterized by UV–visible spectroscopy, X-ray diffraction analysis, Fourier transform infrared spectroscopy, field emission scanning electron microscopy, energy dispersive X-ray analysis and transmission electron microscopy (TEM). The synthesized gold bionanoparticles were spherical in shape with an average of 11.57 ± 1.24 nm as determined by TEM and dynamic light scattering (DLS) particle size analyzer, respectively. The biosynthesized gold nanoparticles exhibited good antimicrobial activity against pathogenic microorganisms. It showed strong antioxidant activity as well as cytotoxicity against HeLa cervical cancer cell line. The present study demonstrated the potential use of the marine actinobacterial strain of *Nocardiopsis* sp. MBRC-48 as an important source for gold nanoparticles with improved biomedical applications including antimicrobial, antioxidant as well as cytotoxic agent.

Keywords Gold bionanoparticles · Extracellular · Marine actinobacteria · Biosynthesis · Antimicrobial · Antioxidant · Cytotoxicity

Introduction

Marine bio-nanotechnology is one of the fastest growing interdisciplinary fields of research interlacing bionanoscience, biomaterial science and technology, with an exponential progress in biomedical applications such as imaging, diagnostics, drug delivery and therapeutics using metal nanoparticles [1–3]. Recent studies of marine microorganisms in the synthesis of nanoparticles are an exciting and upcoming area of research with considerable potential for development [4]. Increasing awareness towards bionanomaterials and other biological processes has led to the development of simple, eco-friendly and novel biological approaches towards the synthesis of advanced bionanomaterials [5]. Even though many biotechnological applications including remediation of toxic metals employ microorganisms, such as bacteria [6], fungi [7] and actinobacteria [8], it is only recently that biomaterials researchers have proposed marine microorganisms as possible eco-friendly nanofactories for biosynthesis of nanoparticles such as gold [9] and silver [8, 10].

Recently, gold bionanoparticles have become the focus of intensive research owing to their wide range of biological and biomedical applications including catalysis, optics, antimicrobials, and the biomaterial production [11]. The marine microbial-mediated synthesis of bionanomaterials has recently been recognized as a potential source for mining bionanomaterials [12]. Biosynthesis of gold nanoparticles using bacteria, actinobacteria, fungi and plants [6–8, 13] are already well documented. However, exploration

P. Manivasagan · M. S. Alam · K.-H. Kang · S.-K. Kim (✉)
Department of Marine-Bio Convergence Science and Marine
Bioprocess Research Center, Pukyong National University,
Busan 608-739, Republic of Korea
e-mail: sknkim@pknu.ac.kr; manimaribtech@gmail.com

M. Kwak
Department of Chemistry, Pukyong National University,
Busan 608-737, Republic of Korea

of the marine actinobacteria has recently heightened interest in the biosynthesis of nanoparticles as nanofactories [12]. Recently, actinobacteria isolated from different ecosystems were recognized as potential syntheses of gold and silver bionanoparticles. The biosynthesis and characterization of nanoparticles have only been reported for *Thermomonospora* sp. [9], *Rhodococcus* sp. [14], *Nocardioopsis* sp. [15] and *Streptomyces* sp. [8, 16].

Members of the genus *Nocardioopsis* belong to the phylum *Actinobacteria*, Class *Actinobacteria*, Order *Actinomycetales*, and Family *Nocardiopsaceae* [17]. They are Gram-positive bacteria that have high genomic guanine and cytosine contents. *Nocardioopsis* are very important microorganisms for the production of several antibiotics and enzymes of commercial value [18]. The organism displays certain atypical physiological and metabolic properties that have made it an important actinomycete. On the basis of these features, a large number of research laboratories all over the world have been studying different basic and applied aspects related to this organism. In the previous studies, *Nocardioopsis* sp. exhibited enzyme production ability [19, 20] and extracellular biologically active substance [21] that can play a key role in silver nanoparticle formation [15]. The present study involves the marine *Nocardioopsis* sp.-mediated synthesis of gold nanoparticles for biomedical applications. Interestingly, this is the first report on the synthesis of gold bionanoparticles by *Nocardioopsis* sp. MBRC-48 and its biological applications including antimicrobial, antioxidant and cytotoxic activities.

Materials and methods

Materials

Gold (III) chloride trihydrate ($\text{HAuCl}_4 \cdot 3\text{H}_2\text{O}$) was purchased from Sigma-Aldrich (St. Louis, USA). All media components were purchased from Lab M Limited (Bury, UK). All chemicals were of analytical grade and procured from Sigma-Aldrich (St. Louis, USA).

Isolation of marine actinobacterium

Marine sediment samples were collected from the Busan coast (Lat 35°09'N; Long 129°07'E), South Korea. The sediment samples were dried to minimize the bacterial contaminants. Sediment sample (1 g) was serially diluted (10^5 dilution), and 0.1 ml of the diluted suspension was plated on starch casein agar medium prepared in 50 % sea water to enhance the isolation of actinobacteria. After 7 days of incubation at 28 °C, white, grey and red powdery colonies of actinobacteria formed were isolated and subcultured, and the strain was maintained on the same media.

Screening of gold nanoparticles

In the preliminary screening process, 35 actinobacterial strains were selected and inoculated in 250-ml Erlenmeyer flasks containing sterile starch casein broth prepared with 50 % sea water in a 50-ml conical flask having pH 7.0 ± 0.2 prior to autoclaving, and incubated in the dark on an orbital shaker (180 rpm) for 96 h at 28 °C. After the incubation period, all the cultures were centrifuged at $10,000 \times g$ for 10 min at 4 °C and 5 ml of cell-free supernatant of each strain was exposed to 50 ml of aqueous solution of 1×10^{-3} M $\text{HAuCl}_4 \cdot 3\text{H}_2\text{O}$ in a 250-ml Erlenmeyer flask. After incubation (180 rpm) for 48 h at 35 °C, the flasks were observed for visual color change pinkish, which indicated the biosynthesis of gold nanoparticles [22].

Identification of marine actinobacterium

During the screening process, strain MBRC-48 was found to effectively produce gold nanoparticles. It was identified on the basis of the 16S rDNA gene sequencing. The 16S ribosomal DNA gene was amplified by PCR using the universal primer pair 27 F 5'-AGAGTTTGATCMTGGCTCAG-3' and 1518 R 5'-AAGGAGGTGWTCCARCC-3'. The amplified products were analyzed by electrophoresis in 0.7 % (w/v) agarose gel and purified using DNA extraction kit (RBC, Korea). The 16S rDNA sequencing was done by Macrogen, South Korea. DNA sequence analysis was then performed by BLAST network services at the NCBI. The 16S rRNA gene sequences of the strain MBRC-48 were aligned with reference sequences obtained from GenBank using Clustal X 2.0.11. Phylogenetic tree was generated using the neighbor-joining method with MEGA 6.0 package [23].

Biosynthesis of gold nanoparticles

The actinobacterial synthesis of gold nanoparticles was carried out according to the method described earlier [9, 24] with certain modifications. The strain MBRC-48 was inoculated in 500-ml Erlenmeyer flasks containing sterile starch casein broth prepared with 50 % sea water in a 250-ml conical flask having pH 7.0 ± 0.2 prior to autoclaving, and incubated in the dark on an orbital shaker for 96 h at 28 °C for 180 rpm. After the incubation period, the culture was centrifuged at $10,000 \times g$ for 10 min at 4 °C and 10 ml of cell-free supernatant was exposed to 100 ml of aqueous solution of 1×10^{-3} M $\text{HAuCl}_4 \cdot 3\text{H}_2\text{O}$ in a 500-ml Erlenmeyer flask. These flasks were further incubated in the dark for 48 h at 35 °C for 180 rpm, resulting in pinkish color indicating the formation of gold nanoparticles. The synthesized gold nanoparticles were collected by high-speed centrifugation and washed with double-distilled water and dialyzed against water to get pure gold

nanoparticles. All the experiments were carried out in triplicate and average values have been reported.

Characterization of gold nanoparticles

UV-visible spectral analysis

The color changes of the reaction mixtures are evidence for gold nanoparticles formation. The absorption spectra of the samples were taken using a double-beam UV-visible spectrophotometer (Shimadzu, Model No-UV 1800) from 200 to 800 nm at different time intervals of incubation (12, 24, 36 and 48 h). All the experiments were done in triplicates and the data obtained were analyzed using Origin Pro 9.0 SRO software (OriginLab Corporation, USA).

X-ray diffraction analysis (XRD)

The actinobacterial supernatant containing gold nanoparticles was freeze-dried on the lyophilizer (Freeze dry system SFDSM, Samwon co., Seoul, South Korea) and stored in lyophilized powdered form until used for further characterization. The finely powdered sample was analyzed by an X-ray diffractometer (PHILIPS X'Pert-MPD diffractometer, The Netherlands) and Cu-K α radiation 1.5405 Å over an angular range of 5°–80°, a step size of 0.02, a scan speed of 4 m⁻¹ at 40 kV voltage, and 30 mA current.

Fourier transform infrared spectroscopy (FTIR)

For Fourier transform infrared spectroscopy (FTIR) measurements, the bio-transformed products present in the cell-free supernatant were lyophilized powder and diluted with potassium bromide in the ratio of 1:100. The characterization of functional groups on the surface of gold nanoparticles was performed by Fourier transform infrared spectroscopy (Perkin-Elmer Inc., USA), and the spectra were scanned in the 400–4,000 cm⁻¹ range at a resolution of 4 cm⁻¹.

Field emission scanning electron microscopy

Synthesized gold nanoparticles were mounted on specimen stubs with double-sided adhesive tape coated with platinum in a sputter coater and examined under field emission scanning electron microscopy (FE-SEM) (JSM-6700, JEOL, Japan).

Energy dispersive X-ray analysis (EDXA)

Energy dispersive X-ray (EDXA) spectroscopy analysis was carried out with the SEM instrument equipped with an EDXA detector operated at an accelerating voltage of 20 keV to perform elemental analysis.

Transmission electron microscopy

An ultrasonically dispersed sample of the solution of gold nanoparticles was placed on a carbon grid, dried at room temperature in clean environment and TEM images were obtained using JSM-6700 (JEOL, Japan) microscope at an accelerating voltage of 120 kV.

Antimicrobial activity of gold nanoparticles

The gold nanoparticles synthesized from *Nocardiopsis* sp. MBRC-48 were tested for antimicrobial activity by well diffusion method against pathogenic organisms such as *Bacillus subtilis* (ATCC 6633), *Pseudomonas aeruginosa* (ATCC 27853), *Escherichia coli* (ATCC 10536), *Staphylococcus aureus* (ATCC 6538), *Candida albicans* (ATCC 10231), *Aspergillus niger* (ATCC 1015), *A. fumigates* (ATCC 1022) and *A. brasiliensis* (ATCC 16404). The pure cultures of bacteria and fungi were subcultured on Müller–Hinton broth for bacteria and Sabouraud broth for fungi at 35 and 30 °C on a rotary shaker at 180 rpm. Wells of 6 mm diameter were made on Müller–Hinton agar and Sabouraud agar plates using gel puncture. Each strain was swabbed uniformly onto the individual plates using sterile cotton swabs. Using a micropipette, 50 and 100 µl of the samples of nanoparticles solution were poured onto each of four wells on all plates. After incubation at 35 and 30 °C for 24 and 48 h, the different levels of zone of inhibition were measured. A H₂AuCl₄ aqueous solution and standard antibiotics, such as tetracycline and nystatin were used as controls.

Antioxidant activity

DPPH free radical scavenging assay

The DPPH (1,1-diphenyl-2-picrylhydrazyl) free radical scavenging assay was conducted based on the method of Dipankar and Murugan et al. [25]. Briefly, 1 ml of gold nanoparticles solutions (in ethanol) with different concentrations (50, 100, 150, 200, 250 and 300 µg/ml) were added to 1 ml of 0.1 mM DPPH (in ethanol) solution. The reaction mixture was shaken for 2 min and incubated in the dark for 30 min at room temperature, and the absorbance was recorded at 517 nm. All the measurements were performed in triplicate and the mean ± standard deviation (SD) represented each value measurements. Ethanol and ascorbic acid were used as the blank and the standard, respectively. The lower absorbance of the reaction mixture indicated a higher percentage of scavenging activity. The percentage of inhibition or scavenging of free radicals was determined by the following formula:

$$\% \text{ Inhibition} = [(\text{Control OD} - \text{Sample OD}) / \text{Control OD}] \times 100$$

where the control was prepared as described above without a sample.

Reducing power assay

The reducing power assay was conducted according to the method recommended by Oyaizu [26]. 500 µl of different concentrations (50, 100, 150, 200, 250 and 300 µg/ml) of synthesized gold nanoparticles were separately mixed with 2.5 ml phosphate buffer (0.2 M, pH 6.6) and 2.5 ml of 1 % potassium ferricyanide. The mixture was incubated at 50 °C for 20 min. To this mixture, 2.5 ml of 10 % trichloroacetic acid was added, which was then centrifuged at 3,000 rpm for 10 min. Finally, 2.5 ml of the supernatant solution was mixed with 2.5 ml of distilled water and 0.5 ml FeCl₃ (0.01 %), and the absorbance was measured at 700 nm in a UV–vis spectrophotometer. Ascorbic acid was used as the standard and phosphate buffer was used as the blank solution. An increase in the absorbance of the reaction mixture indicated stronger reducing power. The assays were accomplished in triplicate and the values were expressed as the mean ± standard deviation (SD).

Total antioxidant capacity

The total antioxidant capacity was assayed following the method of Ravi kumar et al. [27]. The synthesized gold nanoparticles were added in a volume of 0.1 ml at different concentrations (50, 100, 150, 200, 250 and 300 µg/ml) to 1 ml of reagent solution (0.6 M sulfuric acid, 28 mM sodium phosphate and 4 mM ammonium molybdate; mixed in a 1:1:1 ratio). The tubes were capped and incubated in a water bath at 95 °C for 90 min. After the solutions were cooled to room temperature, the absorbance of each aqueous solution was measured at 700 nm against a blank (ethanol). Ascorbic acid was used as the standard and the total antioxidant capacity was expressed as equivalents of ascorbic acid. All the measurements were performed in triplicate and the mean ± standard deviation (SD) represented each value measurements.

Cytotoxic activity

Human cervical cancer cell line (HeLa) was obtained from the American Type Culture Collection (ATCC), USA and maintained in Dulbecco's Modified Eagle Medium (DMEM), supplemented with 10 % fetal bovine serum (FBS) with 1 % penicillin–streptomycin antibiotics (Gibco). Cells were cultured at 37 °C in a humidified atmosphere containing 5 % CO₂. HeLa cells were cultured and seeded into 96-well plates approximately as 1×10^4 cells in each

plate and incubated for 24 h. HeLa cells were treated with a series of 50–400 µg/ml concentration of biosynthesized gold nanoparticles along with cell control and gold nanoparticles control (drug control). After 24 h, cells were washed with PBS and then these plates were subjected for MTT assay. MTT (3-(4,5-dimethylthiazol-2-yl)-2,5-diphenyltetrazolium bromide, a yellow tetrazole) was prepared in 0.5 mg/ml concentration. 100 µl of MTT was added to each well and incubated for 4 h. Purple color formazan crystals formed were then dissolved with 100 µl of dimethyl sulphoxide (DMSO). These crystals were observed at 545 nm in a multi-well ELISA plate reader. OD value was subjected to sort-out percentage of viability of using the following formula, OD value of experimental samples (gold nanoparticles) [28].

$$\text{Percentage of cell viability (\%)} = \frac{\text{Sample absorbance}}{\text{control absorbance}} \times 100$$

Measurement of cytomorphological changes in HeLa cells

HeLa cells were treated with different concentrations of synthesized gold nanoparticles and incubated for 24 h at 37 °C in 5 % CO₂ atmosphere. After the incubation of cells, the gross morphological changes in the cells were visualized and photographed under an inverted phase-contrast microscope (CTR6000, Leica, Wetzlar, Germany).

Apoptosis study

Hoechst 33258 stain is a fluorescent dye mainly used to detect the different characteristic features of apoptosis process. In this experiment HeLa cells were treated with 400 µg/ml gold nanoparticles for 24 h, and then the cells were washed with PBS and fixed with methanol:acetone (3:1, v/v) and stained with Hoechst 33258 (5 µg/ml) at 37° C for 20 min. The nuclear morphology was examined under a fluorescence microscope (Leica, Germany) to identify cells undergoing apoptosis.

Statistical analysis

The experiments for each sample were performed three times and the final values were presented as the mean ± standard deviation (SD). The statistical software, SPSS/14 (one way ANOVA), was used to estimate the statistical parameters.

Results and discussion

Isolation and identification of marine actinobacteria

A total of 35 marine actinobacterial strains were isolated from the marine sediment samples collected from the

Busan coast, South Korea and were selected for the biosynthesis of gold nanoparticles' production screening. Among these strains, strain MBRC-48 exhibited good production and was selected for the extracellular synthesis of gold nanoparticles. This isolate was identified and confirmed by the 16S rDNA sequencing. Amplification and sequencing of marine actinobacterial 16S rDNA gene resulted in 1,544-bp-long nucleotide sequence, which has been deposited in NCBI GenBank (Accession Number: KC179799). The sequence was compared using BLAST algorithm and the closely related sequences were selected followed by their analysis using molecular evolutionary computing software MEGA 6.0. The phylogenetic tree was constructed which confirms that strain MBRC-48 exhibited 100 % similarity with *Nocardiopsis* sp. MBRC-48 (Fig. 1a).

Characterization of gold nanoparticles

UV-visible spectral analysis

Biosynthesis of gold nanoparticles from 10^{-3} M aqueous HAuCl_4 in the presence of *Nocardiopsis* sp. MBRC-48 culture supernatant was observed by UV-Vis spectroscopy. The synthesis of gold nanoparticles was evidenced through the appearance of intense pinkish color due to the reduction

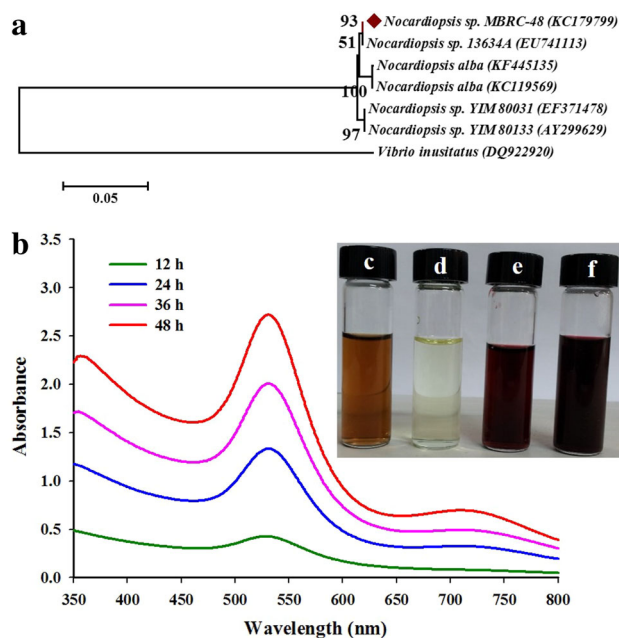


Fig. 1 **a** Phylogenetic tree showing a genetic relationship between the isolate and *Nocardiopsis* sp. MBRC-48 and other closely related reference strains. The scale bar represents 0.05 substitutions per nucleotide position. **b** UV-Vis absorption spectrum of biosynthesized gold nanoparticles. **c** Culture supernatant. **d** Chloroauric acid solution. **e, f** Color change from pinkish color in synthesized gold nanoparticles incubated for 36 and 48 h, respectively

of Au^+ ions, which reached saturation within 48 h of reaction and formed as stable gold nanoparticles (Fig. 1b). These results indicated that the reaction solution has an absorption peak at 530 nm attributed to the surface plasmon resonance band of the gold nanoparticles. Such visual observations on a change in biomass color due to the synthesis of gold nanoparticles have been reported earlier [24, 29, 30].

X-ray diffraction analysis (XRD)

The XRD spectra of the synthesized gold nanoparticles are shown in Fig. 2a. XRD analysis of the nanoparticles showed intense peaks corresponding to (1 1 1), (2 0 0), (2 2 0) and (3 1 1); Bragg's reflection ($2\theta = 38.13^\circ, 44.48^\circ, 64.59^\circ$ and 77.61°) based on the face-centered cubic structure of gold nanoparticles; and that the XRD pattern was compared with a gold standard (Fig. 2b). The broadening of Bragg's peaks indicates the formation of nanoparticles. The mean size of gold nanoparticles was calculated using the Debye-Scherrer's equation by

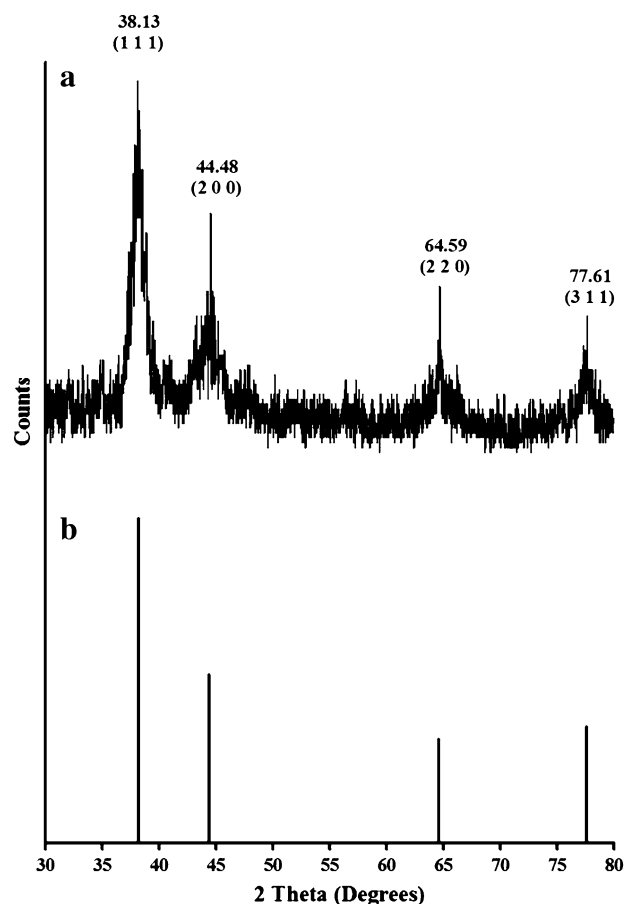


Fig. 2 **a** XRD pattern of synthesized gold nanoparticles using *Nocardiopsis* sp. MBRC-48-mediated biological process with **b** standard

determining the width of the (1 1 1) Bragg's reflection [31]. Earlier studies have also reported the crystalline nature of biosynthesized gold nanoparticles using actinobacteria [9, 24].

Fourier transform infrared spectroscopy (FTIR)

FTIR spectroscopy was used to characterize the functional groups which may play an important role in stabilizing the nanoparticles. FTIR spectra of the culture supernatant and the synthesized gold nanoparticles, as shown in Fig. 3a, can offer information regarding the chemical change of the functional groups involved in the reduction. The FTIR spectrum of the culture supernatant showed band at 3,415, 2,924, 2,858, 2,358, 1,637, 1,384 and 1,052 cm^{-1} . The strong broad absorbance at 3,415 cm^{-1} is the characteristic of the hydroxyl functional group in alcohols and phenolic compounds. The band at 2,924 cm^{-1} can be assigned to the functional group in alkanes. The FTIR spectrum of the gold nanoparticles showed bands at 3,431, 2,937, 1,643, 1,462 and 1,031 cm^{-1} . The band at 3,431 cm^{-1} corresponds to the hydroxyl functional group in alcohols and phenolic compounds. The band at 2,937 cm^{-1} corresponds to the C–H stretch of alkanes. The band at 1,643 corresponds to the $\text{C}=\text{C}$ stretch of alkenes. The band at 1,462 cm^{-1} can be assigned to the C–H bend carbonyl groups and alkanes. The medium bands at 1,031 cm^{-1} correspond to the C–N stretch of the aliphatic amines group. These results indicate that the gold nanoparticles synthesized using *Nocardiopsis* sp. MBRC-48 culture supernatant are surrounded by some proteins, enzymes and metabolites. A previous report reveals that the hydroxyl group (O–H) has a strong ability to interact with nanoparticles [32].

Field emission scanning electron microscopy

FE-SEM determinations of the above-mentioned sample showed the formation of gold nanoparticles, which were confirmed to be the gold by EDXA. EDXA spectroscopy confirmed the presence of elemental gold peak as a major signal (Fig. 3b). Other peaks corresponding to Cl, K and O were also observed, which are possibly due to emissions from macromolecules like proteins/enzymes bound to the nanoparticles or in the vicinity of the particles.

Transmission electron microscopy

A representative TEM image is shown in Fig. 4a. TEM measurements were used to determine the morphology and shape of gold nanoparticles. Low-magnification TEM image revealed that the particle are spherical in shape and non-uniformly distributed (polydispersed) without significant agglomeration. The particle size histogram of gold

nanoparticles shows that the particles size ranges from 7 to 15 nm with an average particle size of 11.57 ± 1.24 nm. The frequency distribution observed from the histogram shows that almost 90 % of the gold nanoparticles are in the 9–13 nm range. These results are in agreement with the values obtained by dynamic light scattering (DLS) measurements as shown in Fig. 4b. Zonooz et al. [33] reported the extracellular biosynthesis of gold nanoparticles by *Streptomyces* sp. ERI-3 cell-free supernatant and the particle size ranged from 10 to 30 nm with spherical shape at the optimum conditions.

Antimicrobial activity of gold nanoparticles

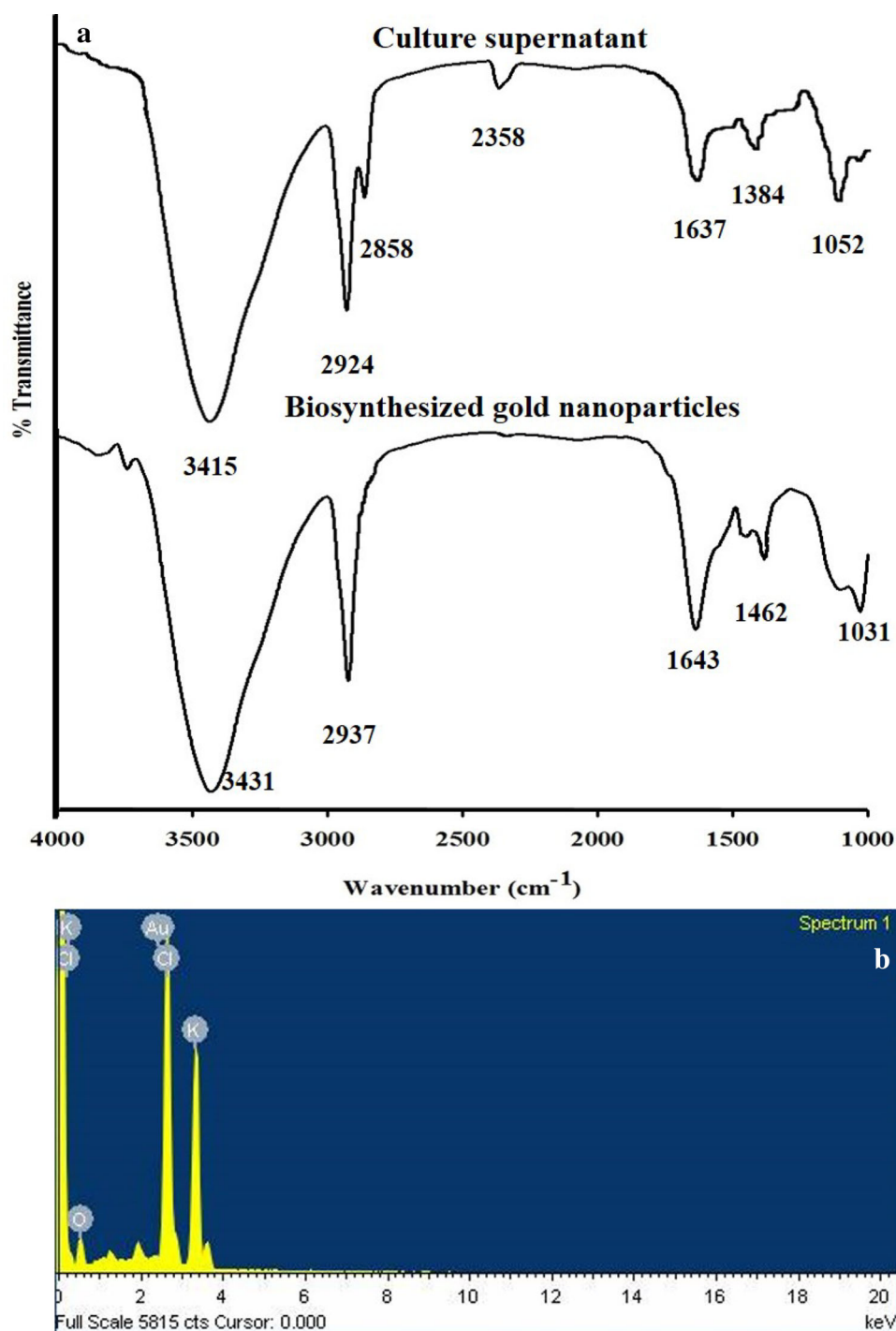
The antimicrobial study of the nanomaterials was performed because of the increase in new strains of microbes that are resistant to most potent antibiotics resulting in new research into the well-known activity of gold and gold-based compounds including gold nanoparticles. This effect was the size and dose dependent, and more pronounced against bacteria and fungi [13]. The antimicrobial activity of gold nanoparticles was investigated against various pathogenic microorganisms such as *Bacillus subtilis* (ATCC 6633), *Pseudomonas aeruginosa* (ATCC 27853), *Escherichia coli* (ATCC 10536), *Staphylococcus aureus* (ATCC 6538), *Candida albicans* (ATCC 10231), *Aspergillus niger* (ATCC 1015), *A. fumigates* (ATCC 1022) and *A. brasiliensis* (ATCC 16404) using well diffusion method. Only the gold nanoparticles that exhibited significant antimicrobial activities compared to HAuCl_4 aqueous solution and standard antibiotics, such as tetracycline and nystatin, are shown in Fig. 5. The highest antimicrobial activity was observed against *Staphylococcus aureus* and *Candida albicans*. These findings are in agreement with previous studies that examined the antibacterial activity of gold nanoparticles against *Enterococcus faecalis* and *Staphylococcus epidermidis* [34, 35]. Khademi Mazdeh et al. [36] reported the biosynthesis of gold nanoparticles using *Escherichia coli* and conjugation with streptomycin and evaluation of its antibacterial activity.

Antioxidant activity

DPPH free radical scavenging assay

DPPH is a stable compound and will be reduced by accepting the hydrogen or electrons. The reducing activity of gold nanoparticles and ascorbic acid was quantified spectrophotometrically by changing the DPPH color from purple to yellow. Percent of inhibition of DPPH radical scavenging activity is presented in Fig. 6a. The DPPH activity of the gold nanoparticles was found to increase in a dose-dependent manner. The results obtained in the DPPH

Fig. 3 **a** FTIR spectra of *Nocardiopsis* sp. MBRC-48 culture supernatant and biosynthesized gold nanoparticles. **b** EDXA spectrum of synthesized gold nanoparticles by *Nocardiopsis* sp. MBRC-48



assay showed effective free radical inhibition by biosynthesized gold nanoparticles. The average percentage inhibition of biosynthesized gold nanoparticles was 69 % as compared to the standard (ascorbic acid). The literature review revealed that the antioxidant activity of the biosynthesized using *Nocardiopsis* sp. MBRC-48 has not been previously performed. Similar observations with the enhanced DPPH scavenging activity by *Solanum nigrum*

leaf extract-mediated gold nanoparticles have been reported [37].

Reducing power assay

Figure 6b shows the dose–response bar chart for the reducing powers of the gold nanoparticles. Reducing powers of the gold nanoparticles were found to increase

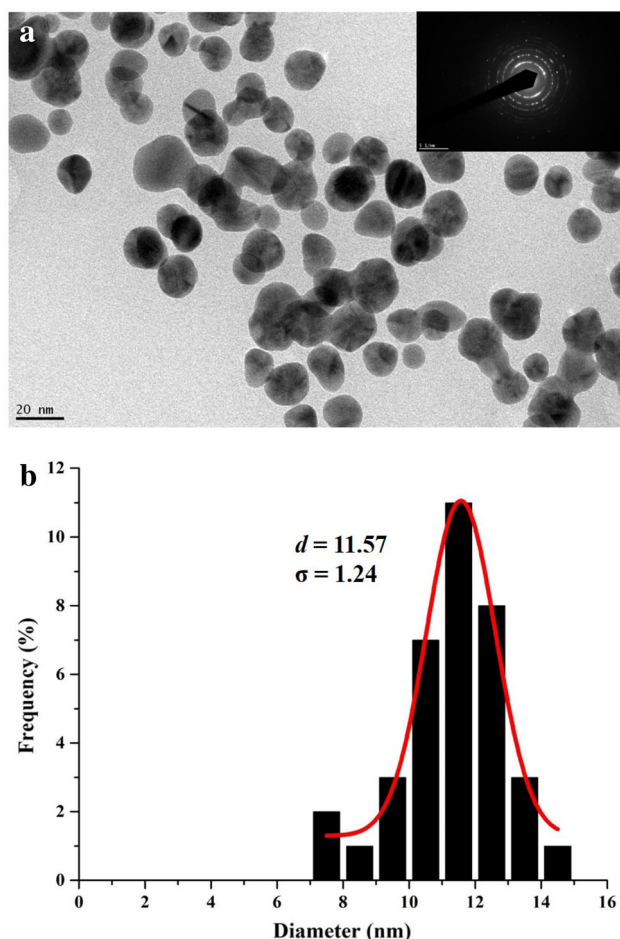


Fig. 4 **a** The TEM images of synthesized gold nanoparticles by *Nocardopsis* sp. MBRC-48 with selected area electron diffraction. **b** DLS histogram of the gold nanoparticle size populations as observed from the TEM image

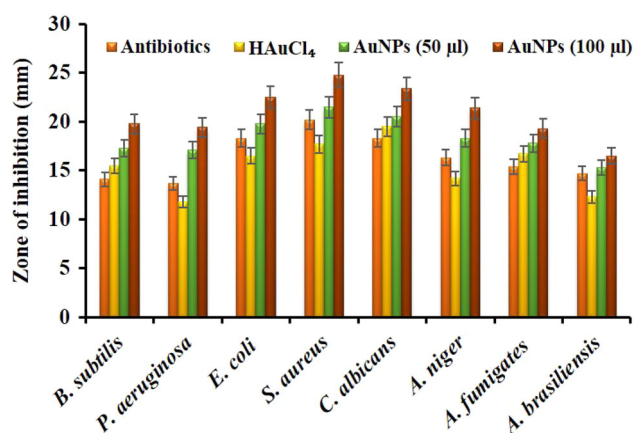


Fig. 5 Antimicrobial activity of gold nanoparticles against pathogenic microorganisms. Error bars mean \pm standard deviation ($n = 3$)

with increasing concentrations. The trend for the gold nanoparticles reducing activity of ferric ion did not differ distinctly from their DPPH free radical scavenging activities. Interestingly, the reducing power was consistently higher than those obtained for DPPH scavenging for the gold nanoparticles. Surprisingly, the gold nanoparticles exhibited comparatively better reducing power than ascorbic acid.

Total antioxidant activity

The antioxidant activity determined using this method differed according to the sample analyzed, but in general, it was also higher in gold nanoparticles thus coinciding with the results of other assays (Fig. 6c). When the absorbance of the gold nanoparticles was compared with that of standard ascorbic acid, the gold nanoparticles were found to possess a higher level of antioxidant activity than ascorbic acid with the highest activity noted in the gold nanoparticles. Superoxide anions are free radicals generated by the transfer of one electron and play an important role in the formation of other reactive oxygen species, such as hydrogen peroxide, hydroxyl radical, or singlet oxygen in living systems [25]. Due to their scavenging power, antioxidants are useful for the management of diseases, such as neurodegenerative diseases, cancer and AIDS.

Cytotoxic activity

The biosynthesized gold nanoparticles were evaluated for their effect on cell viability against human cervical cancer cell line (HeLa) at different concentrations. The biosynthesized gold nanoparticles showed a dose dependent decrease in cell viability. Increase in the time of incubation showed a further decrease in cell viability. Approximately 50 % inhibition of cell viability was seen with gold nanoparticles at 300 $\mu\text{g}/\text{ml}$ (Fig. 7). The results suggested that the biosynthesized gold nanoparticles were very sensitive when compared to control cell. Previously, synthesized gold nanoparticles inducing cytotoxicity were discussed by Mukherjee et al. [1].

Cytomorphology observation

Microscopic observations were monitored using Leica inverted phase-contrast microscope wherein treated cells showed distinct cellular morphological changes indicating unhealthy cells, whereas the control appeared normal (Fig. 8a). Control cells were irregular confluent aggregates with rounded and polygonal cells. Biosynthesized gold

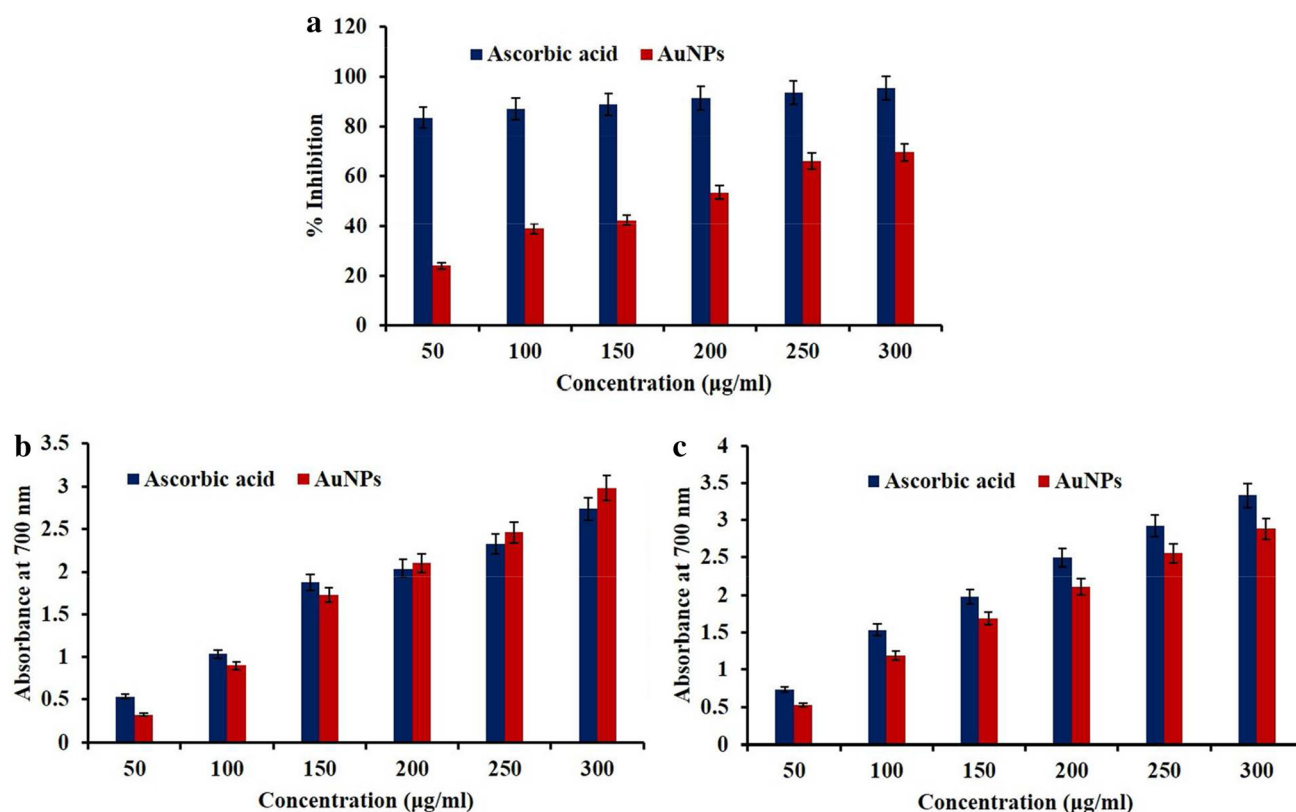


Fig. 6 Antioxidant activity of gold nanoparticles. **a** DPPH free radical scavenging assay of the gold nanoparticles and ascorbic acid. **b** The reducing power assay of the gold nanoparticles and ascorbic

acid. **c** Total antioxidant assay of the gold nanoparticles and ascorbic acid. Error bars mean \pm standard deviation ($n = 3$)

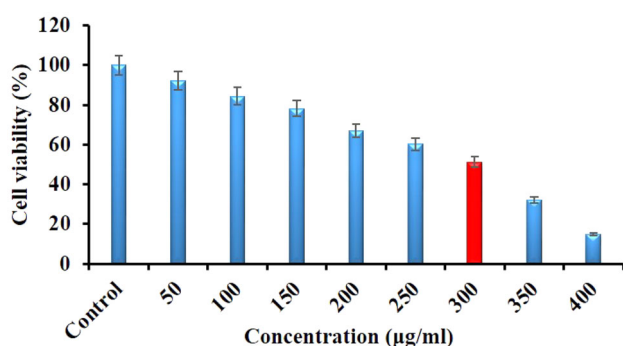


Fig. 7 In vitro cytotoxicity of gold nanoparticles against HeLa cell line. All the data were expressed in mean \pm standard deviation ($n = 3$)

nanoparticles treated cells appeared to shrink and became spherical in shape, and cell spreading patterns were restricted when compared with control. The experimental results clearly proved the excellent anticancer activity of gold nanoparticles against the HeLa cell line. Fascinatingly, previous studies reported the synthesized gold nanoparticles inducing an excellent cytotoxic result against HeLa cancer cell lines at different concentrations [38].

Apoptosis assays

The apoptosis was noticed with the morphological changes in the cell shape and chromatin condensation. In Hoechst staining, after the treatment with 300 μg/ml gold nanoparticles for 24 h, HeLa cells commence to exhibit apoptotic characteristics such as cell shrinkage, nuclear condensation, and fragmentation. In the control group, the cells were regular in morphology and showed an intact nuclear architecture (Fig. 8b). These morphological changes may be due to the activation of caspase cascades, which cleaves the specific substrates responsible for the DNA repair activation. Fascinatingly, earlier studies reported nuclear fragmentation in gold nanoparticle-treated cells [39]. This result clearly indicates that synthesized gold nanoparticles induced apoptosis in HeLa cells. It should be noted that the Hoechst staining clearly indicates the cytotoxicity of gold nanoparticles of cancer cells.

Conclusion

The present study determined that the marine actinobacterium *Nocardopsis* sp. MBRC-48 is an excellent

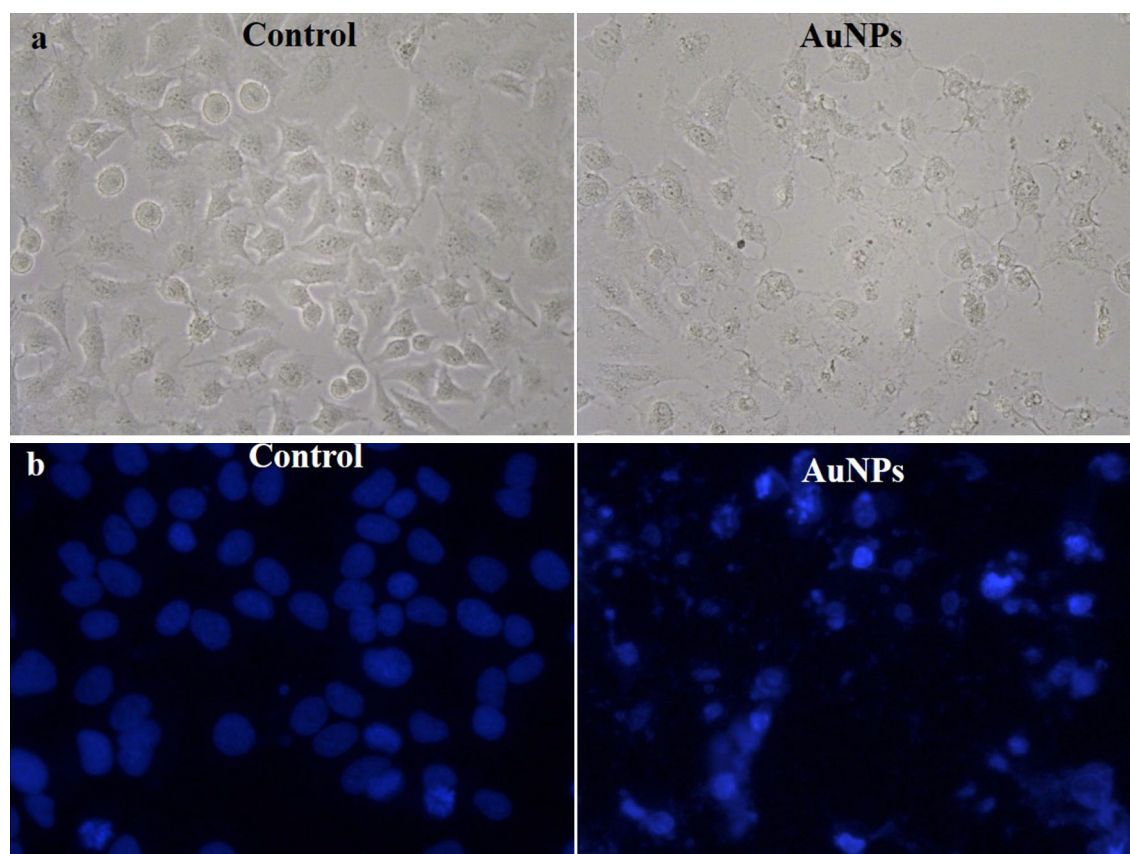


Fig. 8 **a** Phase-contrast microscopic images of HeLa cell line at different concentrations of gold nanoparticle-treated cells and control without gold nanoparticles. **b** Hoechst staining shows apoptotic

bodies and necrotic cell death due to the cytotoxicity of biosynthesized gold nanoparticles at $\times 20$ magnification

microbial resource for the biosynthesis of gold nanoparticles with various biomedical applications such as antimicrobial, antioxidant and anticancer activities. This method is green, inexpensive, environmentally friendly and highly recommended to be used in large-scale production of gold nanoparticles. The biosynthesized gold nanoparticles were thoroughly characterized by several physico-chemical techniques. The particle size distribution of the gold nanoparticles ranges from 7 to 15 nm with an average particle size of 11.57 ± 1.24 nm. To date, there have been no reports on the antimicrobial, antioxidant and cytotoxic activities of gold nanoparticles using marine actinobacterium *Nocardopsis* sp. MBRC-48. The data represented in our study contribute to a new and unexplored area of nanomaterials as alternative medicine. Therefore, further in vivo studies and clinical-level trials are needed to address the formulation of biosynthesized gold nanoparticles and the mechanisms involved with the antimicrobial, antioxidant, and anticancer activities of these particles.

Acknowledgments This paper was supported by research funds of Pukyong National University in 2015.

References

1. Mukherjee S, Sushma V, Patra S, Barui AK, Bhadra MP, Sreedhar B, Patra CR (2012) Green chemistry approach for the synthesis and stabilization of biocompatible gold nanoparticles and their potential applications in cancer therapy. *Nanotechnology* 23:455103–455113
2. Narayanan KB, Sakthivel N (2010) Phytosynthesis of gold nanoparticles using leaf extract of *Coleus amboinicus* Lour. *Mater Character* 61:1232–1238
3. Karthik L, Kumar G, Kirthi AV, Rahuman A, Rao KB (2014) *Streptomyces* sp. LK3 mediated synthesis of silver nanoparticles and its biomedical application. *Bioprocess Biosyst Eng* 37:261–267
4. Kathiresan K, Manivannan S, Nabeel M, Dhivya B (2009) Studies on silver nanoparticles synthesized by a marine fungus, *Penicillium fellutanum* isolated from coastal mangrove sediment. *Coll Surf B* 71:133–137
5. Hsiao M-T, Chen S-F, Shieh D-B, Yeh C-S (2006) One-pot synthesis of hollow Au_3Cu_1 spherical-like and biomineral botallackite $\text{Cu}_2(\text{OH})_3\text{Cl}$ flowerlike architectures exhibiting antimicrobial activity. *J Phy Chem B* 110:205–210
6. Kalishwaralal K, Deepak V, Ram Kumar Pandian S, Gurunathan S (2009) Biological synthesis of gold nanocubes from *Bacillus licheniformis*. *Bioresour Technol* 100:5356–5358
7. Jain N, Bhargava A, Majumdar S, Tarafdar J, Panwar J (2011) Extracellular biosynthesis and characterization of silver

- nanoparticles using *Aspergillus flavus* NJP08: a mechanism perspective. *Nanoscale* 3:635–641
8. Sadhasivam S, Shanmugam P, Yun K (2010) Biosynthesis of silver nanoparticles by *Streptomyces hygroscopicus* and antimicrobial activity against medically important pathogenic microorganisms. *Coll Surf B* 81:358–362
9. Ahmad A, Senapati S, Islam Khan M, Kumar R, Sastry M (2003) Extracellular biosynthesis of monodisperse gold nanoparticles by a novel extremophilic actinomycete, *Thermomonospora* sp. *Langmuir* 19:3550–3553
10. Velmurugan P, Idroose M, Mohideen MHAK, Mohan TS, Cho M, Oh B-T (2014) Biosynthesis of silver nanoparticles using *Bacillus subtilis* EWP-46 cell-free extract and evaluation of its antibacterial activity. *Bioprocess Biosyst Eng* 37:1527–1534
11. Ghaseminezhad SM, Hamed S, Shojaosadati SA (2012) Green synthesis of silver nanoparticles by a novel method: comparative study of their properties. *Carbohydr Poly* 89:467–472
12. Verma V, Kharwar R, Gange A (2009) Biosynthesis of noble metal nanoparticles and their application. *CAB Rev Perspect Agric, Vet Sci, Nutr Nat Resour* 4:1–17
13. Gopinath V, MubarakAli D, Priyadarshini S, Priyadarshini NM, Thajuddin N, Velusamy P (2012) Biosynthesis of silver nanoparticles from *Tribulus terrestris* and its antimicrobial activity: a novel biological approach. *Coll Surf B* 96:69–74
14. Otari S, Patil R, Nadaf N, Ghosh S, Pawar S (2012) Green biosynthesis of silver nanoparticles from an actinobacteria *Rhodococcus* sp. *Mater Lett* 72:92–94
15. Manivasagan P, Venkatesan J, Senthilkumar K, Sivakumar K, Kim S-K (2013) Biosynthesis, antimicrobial and cytotoxic effect of silver nanoparticles using a novel *Nocardiosis* sp. *MBRC-1*. *BioMed Res Inter* 2013:1–9
16. Shanmugasundaram T, Radhakrishnan M, Gopikrishnan V, Pazhanimurugan R, Balagurunathan R (2013) A study of the bactericidal, anti-biofouling, cytotoxic and antioxidant properties of actinobacterially synthesised silver nanoparticles. *Coll Surf B* 111:680–687
17. Sun H, Lapidus A, Nolan M, Lucas S, Del Rio TG, Tice H, Cheng J-F, Tapia R, Han C, Goodwin L (2010) Complete genome sequence of *Nocardiosis dassonvillei* type strain (IMRU 509T). *Stand Genomic Sci* 3:325–336
18. Manivasagan P, Venkatesan J, Sivakumar K, Kim S-K (2014) Pharmaceutically active secondary metabolites of marine actinobacteria. *Microbiol Res* 169:262–278
19. Cavalcanti M, Teixeira M, Lima Filho J, Porto A (2004) Partial purification of new milk-clotting enzyme produced by *Nocardiosis* sp. *Bioresour Technol* 93:29–35
20. Stamford T, Stamford N, Coelho L, Araujo J (2001) Production and characterization of a thermostable α -amylase from *Nocardiosis* sp. endophyte of yam bean. *Bioresour Technol* 76:137–141
21. Kamala K, Sivaperumal P, Gobalakrishnan R, Swarnakumar N, Rajaram R (2014) Isolation and characterization of biologically active alkaloids from marine actinobacteria *Nocardiosis* sp. NCS1. *Biocatalysis Agri. Biotech.* doi:10.1016/j.Bcab.10.005
22. Senapati S, Ahmad A, Khan MI, Sastry M, Kumar R (2005) Extracellular biosynthesis of bimetallic Au–Ag alloy nanoparticles. *Small* 1:517–520
23. Tamura K, Stecher G, Peterson D, Filipski A, Kumar S (2013) MEGA6: Molecular Evolutionary Genetics Analysis Version 6.0. *Mole Biol Evol* 30:2725–2729
24. Vinay Gopal J, Thenmozhi M, Kannabiran K, Rajakumar G, Velayutham K, Abdul Rahuman A (2012) Actinobacteria mediated synthesis of gold nanoparticles using *Streptomyces* sp. VITDDK3 and its antifungal activity. *Materials Lett* 93:360–362
25. Dipankar C, Murugan S (2012) The green synthesis, characterization and evaluation of the biological activities of silver nanoparticles synthesized from *Iresine herbstii* leaf aqueous extracts. *Coll Surf B* 98:112–119
26. Oyaizu M (1986) Antioxidative activities of browning reaction prepared from glucosamine. *Jpn J Nut* 44:307–315
27. Ravikumar Y, Mahadevan K, Kumaraswamy M, Vaidya V, Manjunatha H, Kumar V, Satyanarayana N (2008) Antioxidant, cytotoxic and genotoxic evaluation of alcoholic extract of *Polyalthea cerasoides* (Roxb.) Bedd. *Environ Toxicol Pharmacol* 26:142–146
28. Sukirtha R, Priyanka KM, Antony JJ, Kamalakannan S, Thanagam R, Gunasekaran P, Krishnan M, Achiraman S (2012) Cytotoxic effect of Green synthesized silver nanoparticles using *Melia azedarach* against in vitro HeLa cell lines and lymphoma mice model. *Process Biochem* 47:273–279
29. Karthik L, Kumar G, Bhattacharyya A, Reddy BP, Rao K (2013) Marine Actinobacterial mediated Gold nanoparticles synthesis and their antimalarial activity. *Nanomedicine Nanotechnol Biol Med* 9:951–960
30. Venkatesan J, Manivasagan P, Kim S-K, Kirthi AV, Marimuthu S, Rahuman AA (2014) Marine algae-mediated synthesis of gold nanoparticles using a novel *Ecklonia cava*. *Bioprocess Biosyst Eng* 37:1591–1597
31. Borchert H, Shevchenko EV, Robert A, Mekis I, Kornowski A, Grübel G, Weller H (2005) Determination of nanocrystal sizes: a comparison of TEM, SAXS, and XRD studies of highly monodisperse CoPt3 particles. *Langmuir* 21:1931–1936
32. Talat M, Singh AK, Srivastava O (2011) Optimization of process variables by central composite design for the immobilization of urease enzyme on functionalized gold nanoparticles for various applications. *Bioprocess Biosyst Eng* 34:647–657
33. Zonooz NF, Salouti M, Shapouri R, Nasseryan J (2012) Biosynthesis of gold nanoparticles by *Streptomyces* sp. ERI-3 supernatant and process optimization for enhanced production. *J Cluster Sci* 23:375–382
34. Sadhasivam S, Shanmugam P, Veerapandian M, Subbiah R, Yun K (2012) Biogenic synthesis of multidimensional gold nanoparticles assisted by *Streptomyces hygroscopicus* and its electrochemical and antibacterial properties. *Biometals* 25:351–360
35. Mohanta YK, Behera SK (2014) Biosynthesis, characterization and antimicrobial activity of silver nanoparticles by *Streptomyces* sp. SS2. *Bioprocess Biosyst Eng* 37:1–7
36. Mazdeh SK, Motamedi H, Khiavi AA, Mehrabi MR (2014) Gold nanoparticle biosynthesis by *E. coli* and conjugation with streptomycin and evaluation of its antibacterial effect. *Current Nanosci* 10:553–561
37. Muthuvel A, Adavallan K, Balamurugan K, Krishnakumar N (2014) Biosynthesis of gold nanoparticles using *Solanum nigrum* leaf extract and screening their free radical scavenging and antibacterial properties. *Biomed Preventive Nut* 4:325–332
38. Lokina S, Suresh R, Giribabu K, Stephen A, Lakshmi Sundaram R, Narayanan V (2014) Spectroscopic investigations, antimicrobial, and cytotoxic activity of green synthesized gold nanoparticles. *Spectrochimica Acta Part A: Mol Biomole Spectrosc* 129:484–490
39. Kang B, Mackey MA, El-Sayed MA (2010) Nuclear targeting of gold nanoparticles in cancer cells induces DNA damage, causing cytokinesis arrest and apoptosis. *J American Chem Soc* 132:1517–1519